

**PHOTOPRODUCTION OF ρ^0 ON HYDROGEN
WITH TAGGED PHOTONS BETWEEN 4 AND 6 GeV**

W. STRUCZINSKI

III. Physikalisches Institut der Technischen Hochschule Aachen

P. DITTMANN, V. ECKARDT *, P. JOOS, A. LADAGE, H. MEYER,
B. NAROSKA and D. NOTZ

Deutsches Elektronen-Synchrotron DESY, Hamburg

J. KNOBLOCH, E. RABE and E. MAIER-REIMER
II. Institut für Experimentalphysik der Universität Hamburg

S. BRANDT, M. GRIMM and D. POLLMANN
Institut für Hochenergiephysik, Heidelberg

I. DERADO, G. KRONSEDER and P. SCHACHT
Max-Planck Institut für Physik und Astrophysik, München

Received 11 July 1972

Abstract: We have measured the reaction $\gamma p \rightarrow p\pi^+\pi^-$ in the DESY 1 m Streamer Chamber. The dominant ρ^0 production is analyzed in terms of various models.

1. INTRODUCTION

Previous studies [1–3] of ρ^0 production in the reaction

$$\gamma p \rightarrow p\pi^+\pi^-, \quad (1)$$

have shown that the $\pi^+\pi^-$ mass distribution is skewed relative to a p-wave Breit-Wigner resonance shape and that the slope of the t -distribution (t is the four-momentum transfer squared from incident to outgoing proton) depends strongly on the effective di-pion mass. The skewing of the ρ^0 shape requires model-dependent background subtraction, thus introducing a significant uncertainty into the determination of the cross section for the channel

$$\gamma p \rightarrow p\rho^0. \quad (2)$$

* Now at Max-Planck Institut für Physik und Astrophysik, München.

We have used three phenomenological models, namely a parametrization of the Breit-Wigner curve [3, 4], an interference model [5] and a simple pomeron exchange model [6]. The resulting cross sections are given in table 2.

2. EXPERIMENTAL SET-UP

A monochromatic e^+ beam (with energy settings of 6.5, 4.3, 3.5 and 2.9 GeV) crossing a 1.2 mm Al radiator produced a bremsstrahlung beam. For each photon in the selected energy region the recoil positron was bent onto a hodoscope of 12 overlapping scintillation counters. This defined 23 energy channels with widths between ± 60 MeV and ± 30 MeV. These channels were calibrated by measuring the energy of e^+e^- pairs produced by the tagged photons in the streamer chamber.

The double-gap streamer chamber [7] was filled with a helium-neon gas mixture at 1 atm and was operated with a 500 kV, 10 nsec pulse. The pulse was supplied by a 14 stage Marx generator and formed by a 0.8 m co-axial Blumlein system. Built into the 22 kG magnet of the DESY bubble chamber, the chamber had a sensitive volume of $100 \times 60 \times (2 \times 16)$ cm³.

A liquid hydrogen target (4 cm in length, 2.6 cm in diameter) was surrounded by a cylindric scintillation counter of 0.3 cm thickness and placed inside the chamber. Two counters in the plane perpendicular to the magnetic field recognized electron pair production. A shower counter was used as flux monitor.

3. ANALYSIS OF THE FILM

Approximately 800 000 photographs were taken, showing a total of 40 000 events on hydrogen and 100 000 events on scintillation material. Part of the film was scanned twice, and the combined scanning efficiency was found to be greater than 99%. In this paper, we are concerned only with the data in the energy region between 4.1 and 6.2 GeV. In this energy region we measured 1701 events of type (1). After three measurements about 5% of the events remained unmeasurable. For the geometric and kinematic reconstruction of the events, the CERN program chain (THRESH, GRIND) was used with minor changes. The vertex reconstruction allowed a complete separation of events produced in hydrogen and the scintillation material. The measurement resolution in space was 250 μ m.

4. CORRECTIONS

A detailed description of the corrections for our triggering biases will be published later. The following major corrections to the data were made: (a) The efficiency of the flux monitor was intensity dependent. Therefore our data were nor-

malized to the total γp cross section [3] of $124.5 \mu\text{b}$ at 5 GeV; (b) the cylindrical target counter was not fully efficient. The loss is topology dependent and amounts to $(12 \pm 2)\%$; (c) hadronic events in which one particle hits one of the pair counters were vetoed. This loss has an average value of $(29 \pm 3)\%$.

5. RESULTS

The cross section for reaction (1) was found to be $20.9 \pm 1.7 \mu\text{b}$, in agreement with previous experiments [1–3]. The dominant feature of reaction (1) is the production of ρ^0 . Fig. 1a shows the $\pi^+\pi^-$ mass distribution and fig. 1b the t -distribution for all events. The double differential cross section $d^2\sigma/dM_{\pi\pi} dt$ for reaction (1) is given in table 1. In order to obtain the cross section for ρ^0 production we used three models:

(a) Modification [3, 4] of the p-wave Breit-Wigner distribution by a factor $(M_\rho/M_{\pi\pi})^{n(t)}$, where $n(t)$ is a free parameter.

(b) An interference model, where the ρ^0 production amplitude interferes with a Drell-type background [5].

(c) A pomeron-exchange model with s -channel γ - ρ helicity conservation [6].

In cases (a) and (b) maximum likelihood fits were made to the events of reaction (1) in 9 t -intervals between $|t|_{\min}$ and $|t| = 0.54 \text{ GeV}^2$, taking into account also $\Delta(1236)$ production and a phase-space background. The results of the fits are given in table 2. The values of the slope and the forward cross sections were obtained assuming an $\exp(At)$ dependence of the ρ -production cross section.

In case (c) the two free parameters of the model, to be determined from experimental data, are the overall normalization g and a mass-independent t -distribution slope a (see ref. [6]). In fitting these parameters we used only the region $0.7 \text{ GeV} < M_{\pi\pi} < 0.8 \text{ GeV}$ and $|t| < 0.3 \text{ GeV}^2$. In this interval about 2% background were subtracted using the prism-plot method [8]. From g and a one can calculate within the pomeron exchange model all interesting quantities of reaction (2). They are given in table 2c. The quoted errors are from the statistical uncertainties of the two fitted parameters a and g only. The extrapolation to the unphysical point $t = 0$ was done by fitting the function $\exp(At + Bt^2)$ in the region $|t| < 0.4 \text{ GeV}^2$ to the calculated differential ρ^0 cross sections $d\sigma/dt$. The $\Delta(1236)$ cross section was obtained by using the prism-plot method [8].

To study the helicity of the $\pi^+\pi^-$ system in reaction (1) the angular distribution of one pion in the $\pi^+\pi^-$ rest system was investigated, with the c.m.s. direction of flight of the $\pi^+\pi^-$ system as polar axis. Fig. 2a shows the helicity density matrix elements for $M_{\pi\pi} < 1.0 \text{ GeV}$, which were obtained from a maximum likelihood fit assuming p-wave dominance. They are consistent with s -channel helicity conservation ($\rho_{00} = \rho_{1-1} = \text{Re } \rho_{10} = 0$) for $|t|$ values below 0.3 GeV^2 . In addition fig. 2b shows $\Sigma Y_2^0(\Omega_i)$ and $\Sigma Y_4^0(\Omega_i)$ as a function of $M_{\pi\pi}$. The sum is taken over all events, and Ω is the decay angle in the s -channel helicity system. The Y_2^0 moment shows the same (skewed) ρ -shape as the cross section, again consistent with a helicity

Table 1
Reaction $\gamma p \rightarrow p\pi^+\pi^-$, $4.1 < E_\gamma < 6.2$ GeV.

$M(\text{GeV}) \backslash t (\text{GeV}^2)$	$ t _{\text{min}} - 0.03$	0.03–0.06	0.06–0.09	0.09–0.12	0.12–0.15
0.32–0.36	0	65 ± 65	0	0	22 ± 22
0.36–0.40	77 ± 77	40 ± 32	0	18 ± 18	18 ± 14
0.40–0.44	150 ± 94	39 ± 31	16 ± 16	12 ± 12	35 ± 22
0.44–0.48	177 ± 111	0	91 ± 49	25 ± 19	6 ± 6
0.48–0.52	138 ± 77	79 ± 35	117 ± 48	10 ± 10	22 ± 22
0.52–0.56	200 ± 99	106 ± 42	111 ± 39	34 ± 22	32 ± 20
0.56–0.60	177 ± 73	91 ± 35	171 ± 53	80 ± 35	26 ± 16
0.60–0.64	177 ± 69	144 ± 42	204 ± 57	120 ± 41	59 ± 25
0.64–0.68	237 ± 82	300 ± 67	200 ± 51	201 ± 50	68 ± 29
0.68–0.72	418 ± 128	405 ± 73	368 ± 73	188 ± 51	125 ± 38
0.72–0.76	585 ± 146	499 ± 81	477 ± 87	348 ± 70	245 ± 56
0.76–0.80	490 ± 145	415 ± 72	326 ± 62	263 ± 58	202 ± 48
0.80–0.84	250 ± 91	242 ± 48	199 ± 44	150 ± 43	133 ± 38
0.84–0.88	30 ± 19	104 ± 34	63 ± 24	83 ± 29	51 ± 23
0.88–0.92	72 ± 43	81 ± 28	32 ± 17	79 ± 30	30 ± 16
0.92–0.96	7 ± 7	14 ± 10	8 ± 8	15 ± 11	32 ± 17
0.96–1.00	0	7 ± 7	8 ± 8	6 ± 6	0
1.00–1.04	0	8 ± 6	33 ± 21	31 ± 16	8 ± 8
1.04–1.08	0	9 ± 9	33 ± 26	9 ± 9	8 ± 8
1.08–1.12	0	0	9 ± 9	17 ± 12	0
1.12–1.16	0	16 ± 11	0	9 ± 9	0
1.16–1.20	0	7 ± 7	0	0	0
1.20–1.28	0	5 ± 5	7 ± 5	4 ± 4	5 ± 5
1.28–1.36	0	4 ± 4	4 ± 4	0	9 ± 9
1.36–1.44	0	0	8 ± 6	9 ± 9	0
1.44–1.52	0	4 ± 4	5 ± 5	12 ± 10	0
1.52–1.60	0	0	0	9 ± 6	10 ± 7
1.60–1.68	0	0	0	0	0
1.68–1.76	0	0	0	0	0
1.76–1.84	0	0	0	0	0
1.84–1.92	0	0	0	0	0
1.92–2.00	0	0	0	0	0
$d\sigma/dt (\mu\text{b}/\text{GeV}^2)$	127 ± 23	108 ± 11	100 ± 11	71 ± 8	47 ± 6

Double differential cross section $d\sigma/dM_{\pi\pi} dt_{pp}$ in $\mu\text{b}/\text{GeV}^3$.

Table 1 (continued).

0.15–0.18	0.18–0.24	0.24–0.30	0.30–0.39	0.39–0.54	0.54–0.80	$d\sigma/dM$ ($\mu\text{b}/\text{GeV}$)
0	0	0	7 ± 4	0	0	3 ± 2
0	0	0	0	0	1 ± 1	5 ± 2
0	9 ± 7	3 ± 3	4 ± 4	0	1 ± 1	9 ± 3
25 ± 20	10 ± 8	0	3 ± 3	0	0	11 ± 4
10 ± 10	10 ± 8	4 ± 4	0	0	1 ± 1	13 ± 3
11 ± 11	8 ± 6	4 ± 4	5 ± 5	0	0	16 ± 4
22 ± 22	13 ± 8	5 ± 5	5 ± 4	0	1 ± 1	20 ± 4
51 ± 23	25 ± 12	9 ± 6	5 ± 3	1 ± 1	1 ± 1	26 ± 4
92 ± 39	31 ± 15	8 ± 6	21 ± 9	3 ± 3	2 ± 1	39 ± 6
151 ± 49	96 ± 25	59 ± 18	28 ± 10	4 ± 2	2 ± 1	64 ± 8
230 ± 54	104 ± 24	76 ± 23	20 ± 8	13 ± 6	4 ± 2	88 ± 9
186 ± 50	91 ± 23	64 ± 20	33 ± 12	23 ± 8	5 ± 3	76 ± 9
27 ± 14	51 ± 19	23 ± 11	27 ± 10	5 ± 3	3 ± 2	40 ± 5
62 ± 26	48 ± 16	30 ± 12	14 ± 8	7 ± 4	4 ± 2	20 ± 3
9 ± 9	12 ± 7	12 ± 7	12 ± 6	0	1 ± 1	12 ± 3
0	14 ± 8	15 ± 9	0	7 ± 4	1 ± 1	6 ± 1
16 ± 12	8 ± 6	4 ± 4	0	0	0	2 ± 1
13 ± 9	9 ± 6	4 ± 4	2 ± 2	9 ± 5	4 ± 2	7 ± 2
0	13 ± 8	0	0	2 ± 2	1 ± 1	4 ± 1
4 ± 4	5 ± 5	4 ± 4	3 ± 3	3 ± 2	0	2 ± 1
30 ± 24	10 ± 7	0	16 ± 8	7 ± 4	0	5 ± 2
0	4 ± 4	0	10 ± 6	3 ± 2	0	2 ± 1
8 ± 6	8 ± 4	6 ± 3	1 ± 1	1 ± 1	1 ± 1	3 ± 1
0	2 ± 2	2 ± 2	2 ± 2	1 ± 1	2 ± 1	2 ± 1
0	6 ± 4	6 ± 4	0	4 ± 2	0	3 ± 1
0	0	6 ± 4	3 ± 3	1 ± 1	0	2 ± 1
2 ± 2	9 ± 5	4 ± 3	3 ± 2	2 ± 1	0	3 ± 1
0	6 ± 6	4 ± 3	5 ± 3	3 ± 2	1 ± 1	2 ± 1
4 ± 4	4 ± 3	0	1 ± 1	2 ± 1	1 ± 1	2 ± 1
0	3 ± 2	4 ± 4	1 ± 1	1 ± 1	2 ± 1	2 ± 1
0	0	0	0	3 ± 2	3 ± 1	1 ± 1
0	0	0	0	2 ± 1	0	1 ± 1
39 ± 6	26 ± 3	16 ± 2	10 ± 2	5 ± 1	2 ± 1	21 ± 2

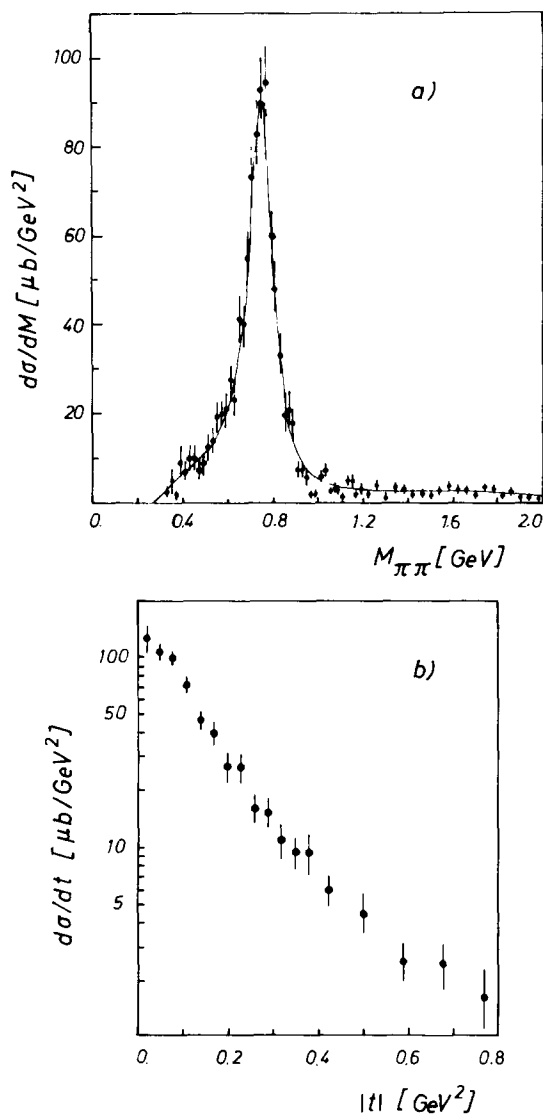


Fig. 1. Reaction $\gamma p \rightarrow p\pi^+\pi^-$, $4.1 < E_\gamma < 6.2$ GeV. a. $d\sigma/dM_{\pi\pi}$ in $\mu\text{b}/\text{GeV}^2$. The curve is a fit with model (a). b. $d\sigma/dt_{pp}$ in $\mu\text{b}/\text{GeV}^2$.

conserving p-wave. The structure in the Y_4^0 moment at $M_{\pi\pi} < M_p$ is suggestive of an interference between diffractive ρ^0 production and a Drell-type background amplitude [5]. It was checked that this structure is not a statistical effect induced by the strongly peaking Y_2^0 moment.

Table 2
 Reaction $\gamma p \rightarrow p\pi^+\pi^-$, $4.1 < E_\gamma < 6.2$ GeV.

Model	$\sigma(\gamma p \rightarrow p\rho^0)$ (μb)	A (GeV^{-2})	B (GeV^{-4})	$\frac{d\sigma(\gamma p \rightarrow p\rho^0)}{dt} \Big _{t=0}$ ($\mu\text{b}/\text{GeV}^2$)	M_ρ (GeV)	Γ_ρ (GeV)	$\sigma(\gamma p \rightarrow \Delta^{++}\pi^-)$ (μb)	$\sigma(\gamma p \rightarrow \Delta^0\pi^+)$ (μb)
(a)	18.1 ± 1.5	8.9 ± 0.4		156 ± 15	0.762	0.133	1.1 ± 0.2	0.4 ± 0.1
(b)	15.2 ± 1.4	8.0 ± 0.5		135 ± 19	0.762	0.133	0.9 ± 0.3	
(c)	17.0 ± 2.0	9.7 ± 0.8	2.3 ± 0.2	159 ± 20	0.765	0.155	1.0 ± 0.15	0.5 ± 0.1

ρ^0 and Δ production cross section in terms of three models.

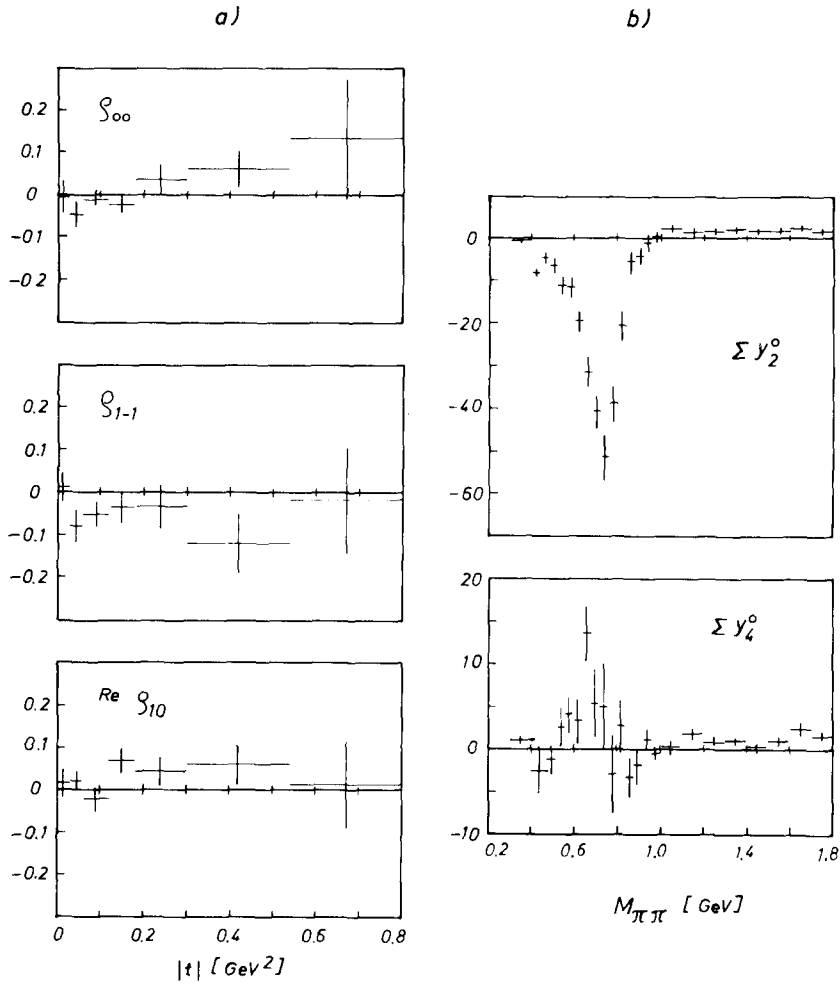


Fig. 2. $4.1 < E_\gamma < 6.2$ GeV. a. Reaction $\gamma p \rightarrow p\rho^0$, density matrix elements of ρ^0 as a function of t_{pp} . b. Reaction $\gamma p \rightarrow p\pi^+\pi^-$, moments $\Sigma Y_2^0(\Omega_i)$ and $\Sigma Y_4^0(\Omega_i)$ as a function of $M_{\pi\pi}$ for $t_{pp} < 0.5$ GeV² (the sum is taken over all events).

We are indebted to G. Horlitz and his group for continuous support of our experiment while the streamer chamber was inside the bubble chamber magnet. We want to thank our scanning and measuring staff for their skillful work. We are grateful to P. Söding and N. Schmitz for many discussions.

REFERENCES

- [1] Aachen-Berlin-Bonn-Hamburg-Heidelberg-München Collaboration, *Phys. Rev.* 175 (1968) 1669.
- [2] Y. Eisenberg et al., *Phys. Rev. D* 5 (1972) 15.
- [3] J. Ballam et al., *Phys. Rev. D* 5 (1972) 545.
- [4] M. Ross and L. Stodolsky, *Phys. Rev.* 149 (1966) 1172.
- [5] P. Söding, *Phys. Letters* 19 (1965) 702.
- [6] I. Derado et al., *Nucl. Phys.* B38 (1972) 541.
- [7] V. Eckardt and A. Ladage, *Proc. of the Symp. on nuclear electronics, Versailles, III*, 10–1, 1968; *Proc. of the Int. Conf. on instrumentation for high energy physics, Dubna, 1970*.
- [8] J.E. Brau et al., *Phys. Rev. Letters* 27 (1971) 1481.